3D Magnetic Field Reconstruction and Mapping with Physics-Informed Neural Networks

Haohan Yu, Zhanxu Hao, Bingzhi Li,
Zejia Lu, Xiang Chen, Liang Li

上海交通大學
SHANGHAI JIAO TONG UNIVERSITY

之江实验室
ZHEJIANG LAB

中国物理学会高能物理分会
HIGH ENERGY PHYSICS BRANCH OF CPS
華南師範大學

中国物理学会高能物理分会
第十二届全国会员代表大会暨学术年会

之江实验室 ZHEJIANG LAB

Outline

之江实验室 ZHEJIANG LAB

Muon g-2/EDM Experiment at J-PARC

The J-PARC E34 experiment requires precise magnetic field across the entire muon beamline:

1. Muon Production Region

preserve polarization during cooling, Ambient field < ±1 μT

2. 3D Injection Scheme

high-precision field for beam transport

3. Storage Ring

Field monitored with sub-ppm stability to suppress systematic uncertainties in spin precession measurements

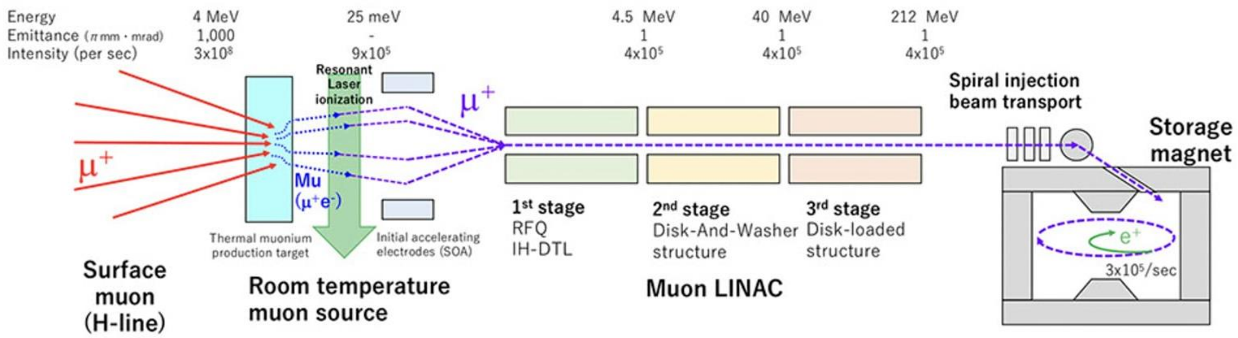

J-PARC muon g-2/EDM experiment beamline schematic

Key Challenge: Reconstruct fields in regions where direct probe placement is obstructed by vacuum chambers or complex detector geometries — requiring advanced interpolation methods that maintain physical consistency.

Multipole expansion method

- The magnetic field vector can be written as a gradient of a scalar magnetic potential function:

$$\boldsymbol{B} = -\nabla\Phi_M(\boldsymbol{r})$$

- The magnetic scalar potential satisfies Laplace's equation:

$$\nabla^2\Phi_M = 0$$

- the solution of Laplace's equation in spherical coordinates is given by:

$$\Phi_M(r,\theta,\phi) = \sum_{l}^{\infty}\sum_{m}^{l} r^l P_l^m(\cos\theta)[a_{lm}\cos(m\phi) + b_{lm}\sin(m\phi)]$$

- where P_l^m are the associated Legendre polynomials, and a_{lm} and b_{lm} are expansion coefficients
- Absorbing a_{lm} and b_{lm} in a coefficient c_n, we can write the magnetic field in a compact form

$$\boldsymbol{B}(x,y,z) = \sum_{n} c_n \boldsymbol{f}_n(x,y,z)$$

➢ B field multipole expansion in the Fermilab muon g-2 experiment

$$B_y = a_0 + \sum_{n=1}^{\infty}(r/r_0)^n[a_n cos(n\theta) + b_n sin(n\theta)]$$

	f_0	f_1	f_2	f_3	f_4	f_5	f_6	f_7	f_8	f_9
x	0	-1	0	$-x$	$-3z$	0	$6x$	$6y$	$-3xz$	$\frac{3}{2}(3x^2+y^2-4z^2)$
y	0	0	-1	$-y$	0	$-3z$	$-6y$	$6x$	$-3yz$	$3xy$
z	1	0	0	$2z$	$-3x$	$-3y$	0	0	$-\frac{3}{2}(x^2+y^2-2z^2)$	$-12xz$

the first 10 f_n basis vector functions

Multipole expansion method

- The magnetic field vector can be written as a gradient of a scalar magnetic potential function:

$$\boldsymbol{B} = -\nabla\Phi_M(\boldsymbol{r})$$

- The magnetic scalar potential satisfies Laplace's equation:

$$\nabla^2\Phi_M = 0$$

Limitation: Expansion must be terminated at finite order for numerical stability, creating truncation errors that restrict resolution.

$$\boldsymbol{B}(x,y,z) = \sum_n c_n \boldsymbol{f}_n(x,y,z)$$

- B field multipole expansion in the Fermilab muon g-2 experiment

$$B_y = a_0 + \sum_{n=1}^{\infty}(r/r_0)^n[a_n cos(n\theta) + b_n sin(n\theta)]$$

	f_0	f_1	f_2	f_3	f_4	f_5	f_6	f_7	f_8	f_9
x	0	-1	0	$-x$	$-3z$	0	$6x$	$6y$	$-3xz$	$\frac{3}{2}(3x^2+y^2-4z^2)$
y	0	0	-1	$-y$	0	$-3z$	$-6y$	$6x$	$-3yz$	$3xy$
z	1	0	0	$2z$	$-3x$	$-3y$	0	0	$-\frac{3}{2}(x^2+y^2-2z^2)$	$-12xz$

the first 10 f_n basis vector functions

PINN Concept & Network Architecture

CONCEPT

Physics-Informed Neural Networks embed Maxwell's equations directly into the neural network's loss function.

Unlike traditional "black-box" deep learning, PINNs enforce physical laws as constraints:

- **Divergence-free**: $\nabla \cdot B = 0$
- **Curl-free**: $\nabla \times B = 0$

Total Loss: L = L_data + L_phys

Physics Loss: enforces Maxwell's equations at collocation points r_f and sensor points r_d

$$L_{phys} = \frac{1}{N}\sum_{j\in\{r_f,r_d\}} \| \nabla \cdot B_{pred}(r_j) \|^2 + \frac{1}{N}\sum_{j\in\{r_f,r_d\}} \| \nabla \times B_{pred}(r_j) \|^2$$

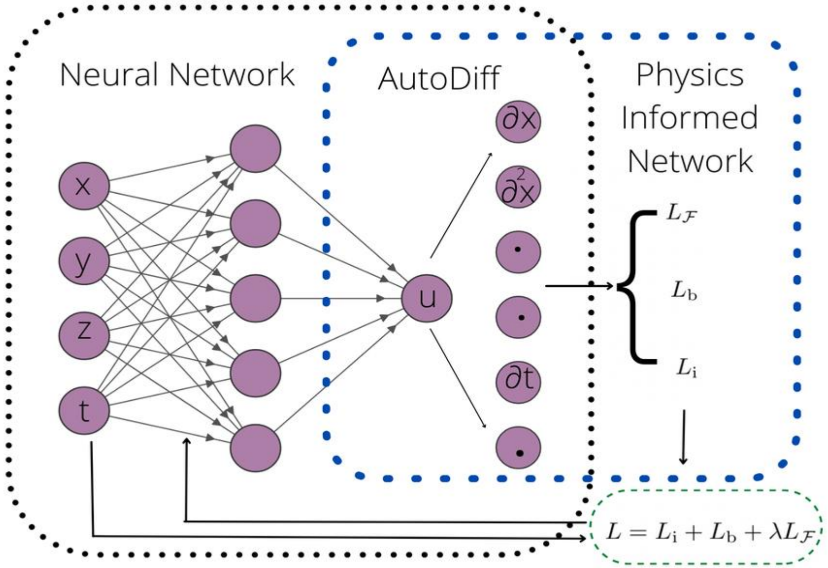

Physics-Informed Neural Network architecture

Input: Position (x, y, z) →

Output: Magnetic Field B = (B_x, B_y, B_z)

之江实验室 ZHEJIANG LAB

Three-Stage Training Strategy

01 AdamW

First-order optimization with **decoupled weight decay**

→

02 LBFGS

Second-order **quasi-Newton method**

→

03 RAR Refinement

Residual-based Adaptive Refinement

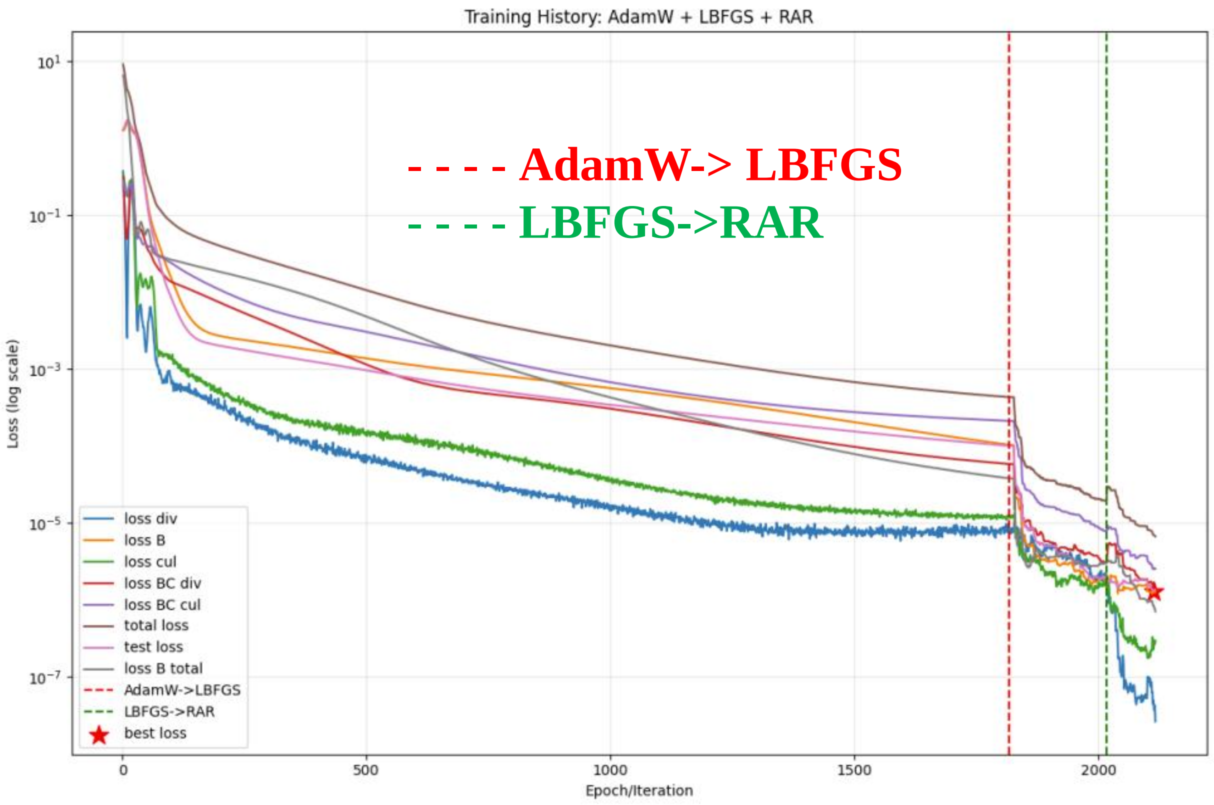

- Divergence-free:

  $\nabla \cdot B$ loss at 10^{-7} level

- Curl-free:

  $\nabla \times B$ loss at 10^{-7} level

Biot-Savart Simulation Result

$$B(r) = \frac{\mu_0}{4\pi} \sum_i I_i \oint \frac{dl_i \times (r - r_i)}{| r - r_i |^3}$$

- Synthetic environment with **multiple current-carrying circular loops** generating field
- Achieve ~10^{-4} relative error despite severely limited training data

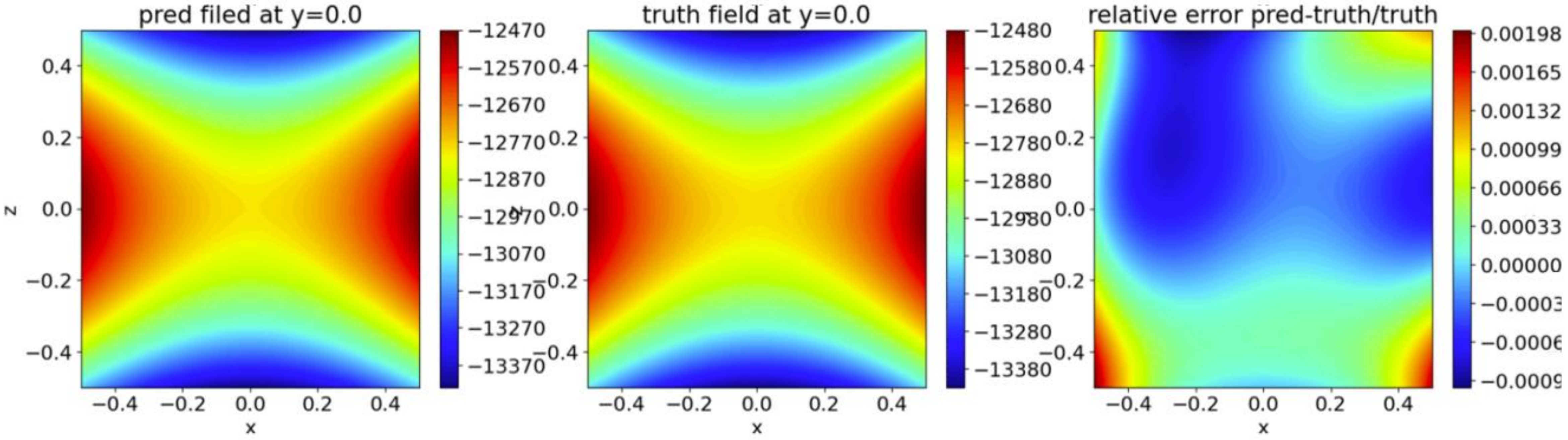

PINN predicted field | Biot-Savart ground truth | Relative error (pred − truth)/truth

Custom Coil Assembly & 3D Mapping System

- High-precision automated **three-axis translation stage**
- Positioning repeatability: **±0.05 mm**

- Three orthogonal **non-standard coil pairs**:

- Two circular pairs (414mm / 440mm diameter)

- One rectangular pair (378×272 mm)

- Generates controllable central field: **0–400 µT**
- J-PARC experimental geometry as the design reference

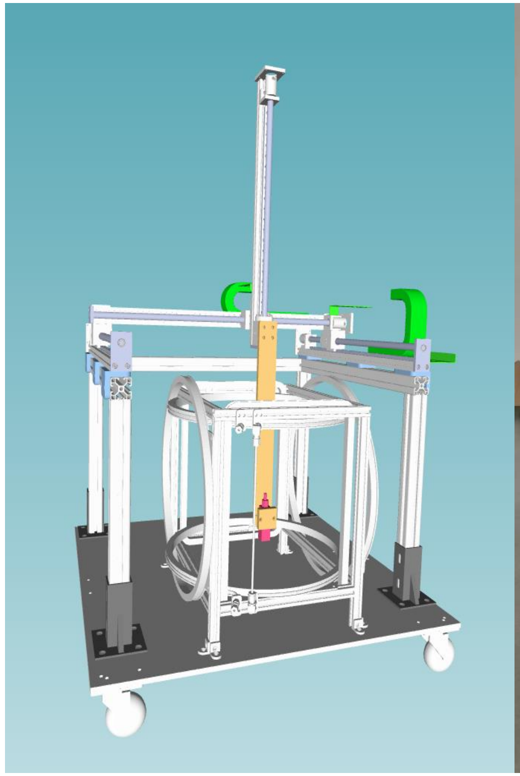

之江实验室 ZHEJIANG LAB

Custom Coil Assembly & 3D Mapping System

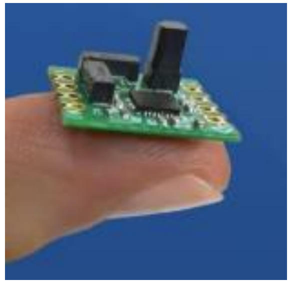

RM3100 magneto-inductive sensor

- Resolution: **13 nT**
- Intrinsic noise floor: **15 nT**
- Measurement range $\pm 1100\ \mu T$

- **10-second dwell time** per point (10 Hz sampling)
- Stable measurement: σ ≈ **30 nT**
- Scan cube: [-80mm, 80mm] at 40mm interval
- 125 points (5×5×5 grid)

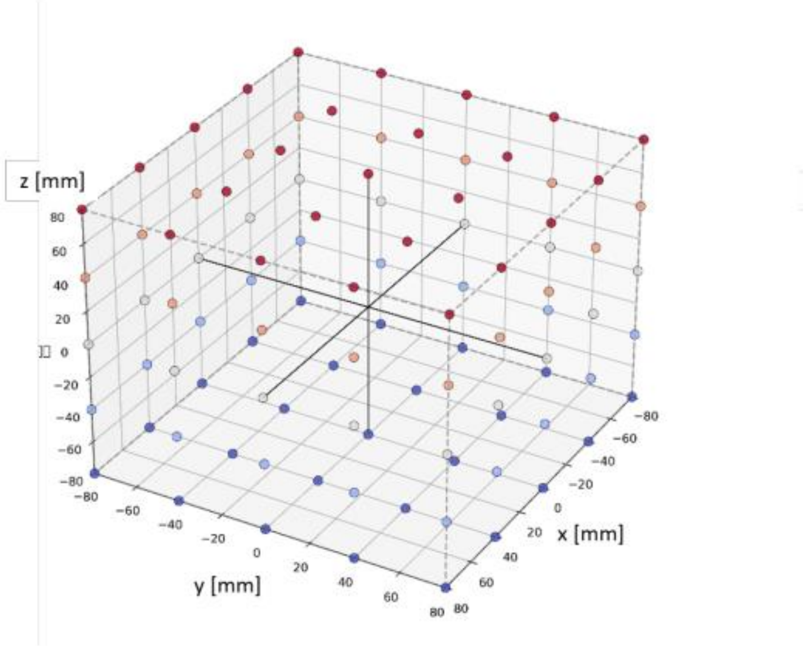

之江实验室 ZHEJIANG LAB

Experimental Performance Across Dynamic Range (0–400 μT)

Table 3. Performance comparison of PINN and multipole methods on experimental magnetic field data across varying central field strengths ($B_0 = 0\text{–}400\ \mu T$) and training point densities (30 and 98 points).

Center B_0 (μT)	$\lvert B \rvert$ Range (μT)	Training Points	PINN (Mean±Std)		Multipole (Mean±Std)	
			Signed Err (μT)	Rel Err (%)	Signed Err (μT)	Rel Err (%)
0	0.123–3.266	30	0.032±0.332	13.337±52.159	0.029±0.609	18.095±65.424
0	0.123–3.266	98	−0.021±0.277	9.399±41.286	0.182±0.910	57.546±197.063
10	7.478–12.400	30	0.050±0.253	0.503±2.520	0.148±0.580	1.749±5.911
10	7.478–12.400	98	−0.014±0.134	−0.109±1.369	−0.549±0.504	−5.328±5.106
100	94.321–107.824	30	−0.119±0.201	−0.114±0.198	−0.750±2.626	−0.678±2.599
100	94.321–107.824	98	0.108±0.151	0.111±0.155	0.066±2.593	0.134±2.591
400	374.210–424.142	30	−0.182±0.804	−0.040±0.204	−4.121±9.108	−0.974±2.261
400	374.210–424.142	98	-0.115±0.363	-0.027±0.091	0.830±8.926	0.260±2.248

- **Sub-μT precision:** PINN mean absolute error ~0.1 μT for most configs
- The best achieved accuracy to **10^{-4} level**
- **Stable predictions:** PINN σ ≪ multipole σ

Reconstruction Precision at B_0 = 400 µT

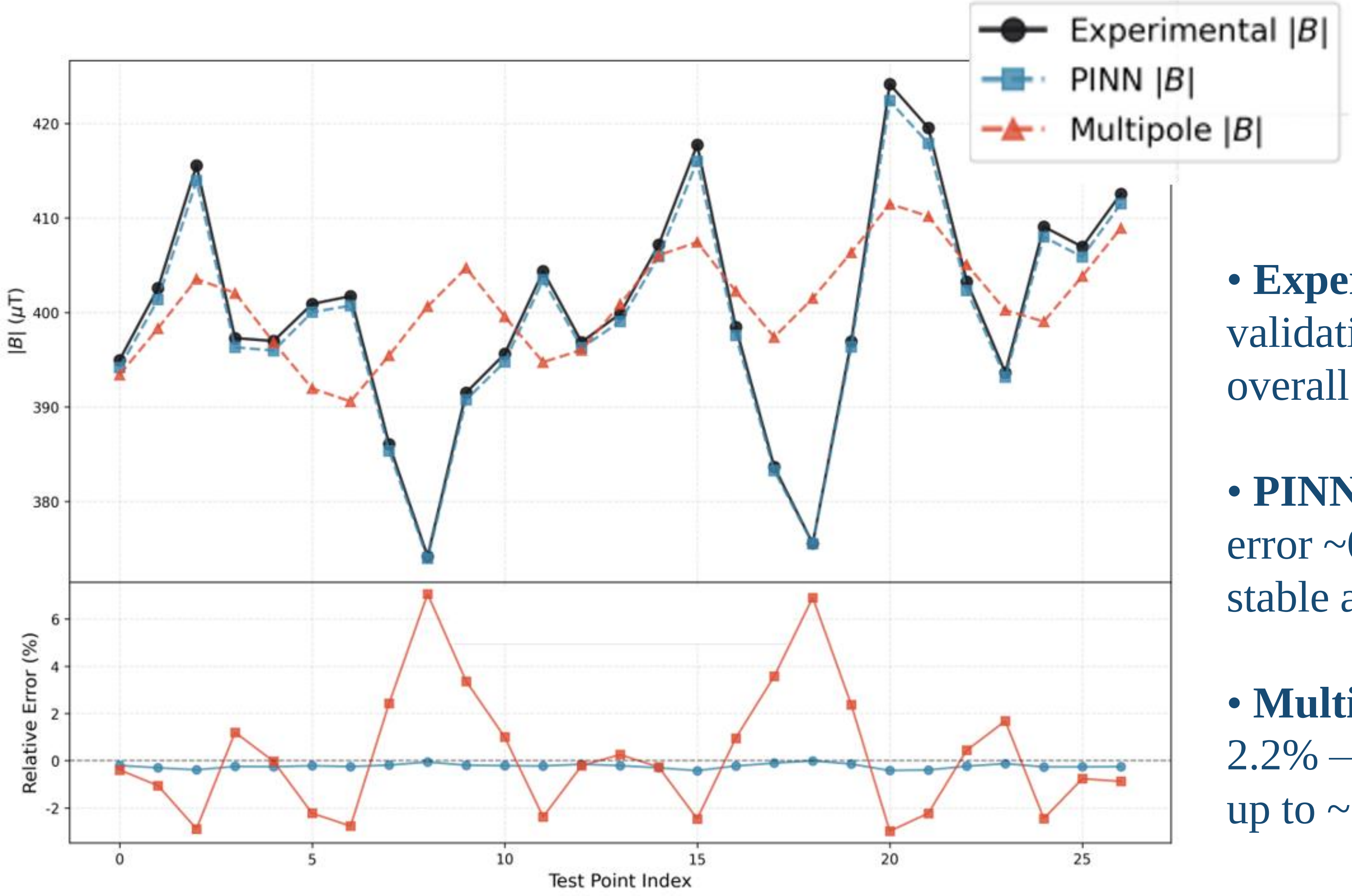

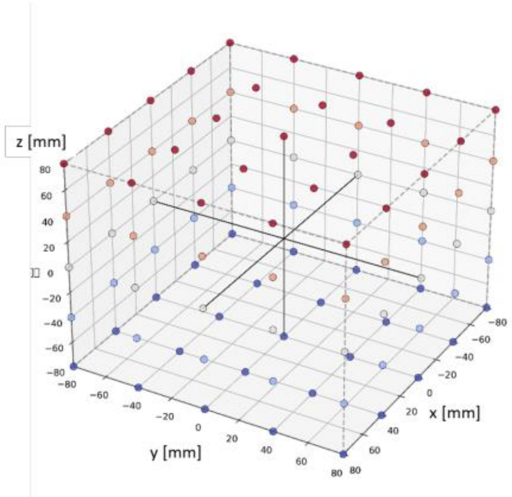

- **Experimental coil test:** interior validation points, both methods capture overall spatial variation
- **PINN** tracks experimental $|B|$ with mean error ~0.03% and $\sigma \approx 0.09\%$ — highly stable across all points
- **Multipole** shows bias (~0.26%) and $\sigma \approx 2.2\%$ — **20× larger variance**, local spikes up to ~6%

之江实验室 ZHEJIANG LAB

Summary

Framework

Physics informed neural network for 3D field reconstruction

Simulation and Experiment

Reconstruction accuracy **~10^{-4} level**

Sub-μT precision across 0–400 μT range

Direct Applications

- **Muon g-2/EDM** requiring field stability
- Mapping in **restricted sensor access** regions
- Vacuum chambers and complex detectors

Advantages Over Traditional Methods

- **Eliminates truncation artifacts** in harmonic expansion
- Avoids **resolution-noise trade-off** of multipole
- No manual tuning of expansion orders

Paper in submission stage, https://arxiv.org/abs/2605.25640

Thank You

Questions & Comments Welcome

Contact: bingzhi.li@zhejianglab.org

liangliphy@sjtu.edu.cn

Affiliation:

Shanghai Jiao Tong University & Zhejiang Lab

Precision Requirements & Scientific Goals

Region / Application	Field Requirement	Key Challenge
Muon Production	Ambient field < ±1 μT	Preserve muonium spin polarization against ~60 μT geomagnetic field
3D Injection	High-precision prediction	Efficient beam transport and matching in complex geometry
Storage Ring (g-2)	Sub-ppm stability	Suppress systematic uncertainties in spin precession

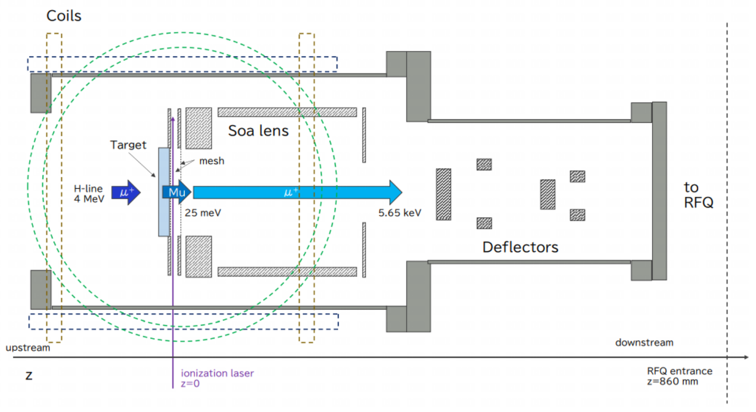

Helmholtz coil configuration for magnetic field control

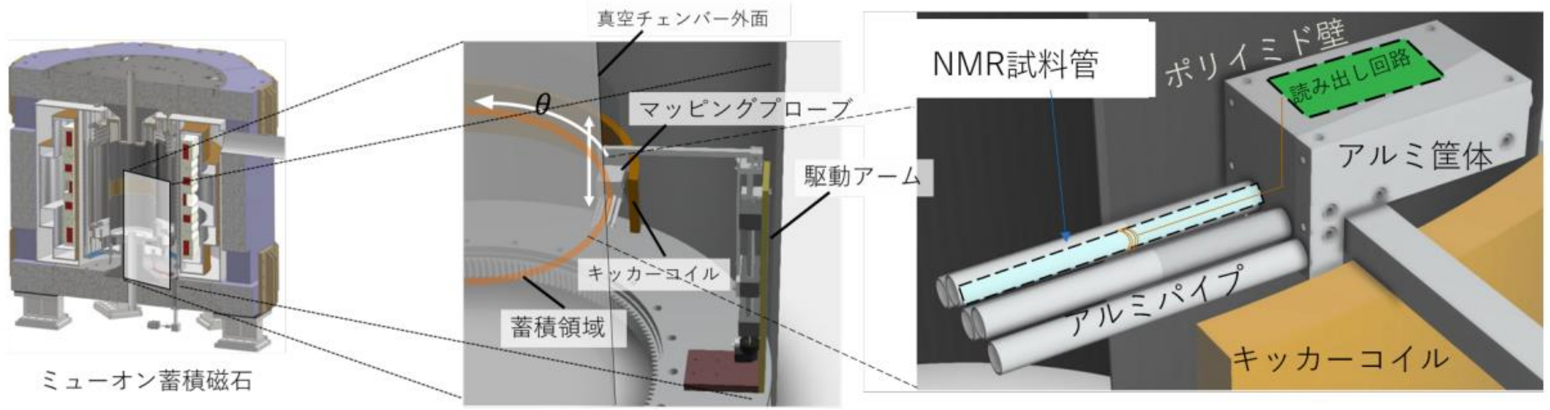

NMR probes for magnetic field measurement

之江实验室 ZHEJIANG LAB

Precision Requirements & Scientific Goals

Region / Application	Field Requirement	Key Challenge
Muon Production	**Ambient field < ±1 μT**	**Preserve muonium spin polarization against ~60 μT geomagnetic field**
3D Injection	**High-precision prediction**	**Efficient beam transport and matching in complex geometry**
Storage Ring (g-2)	**Sub-ppm stability**	**Suppress systematic uncertainties in spin precession**

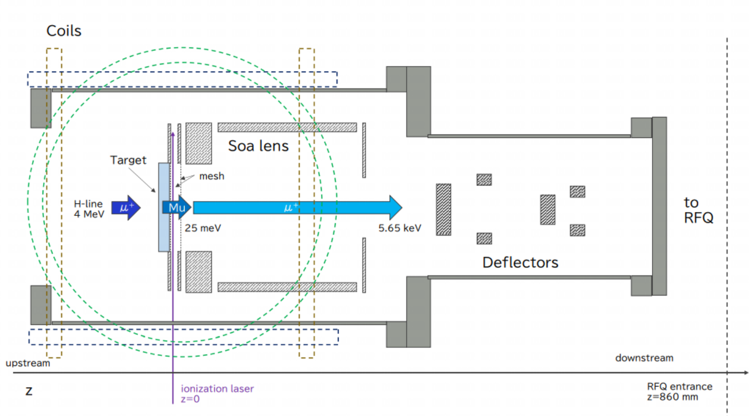

Helmholtz coil configuration for magnetic field control

Functions	Location	Specifications
Main field	$r = 333 \pm 15$ mm, $z = \pm 50$ mm	Axial field (B_{0z}) = 3 T Local uniformity < 1,000 ppb Integrated uniformity along the orbit less than 100 ppb (peak-to-peak)
Injection field	$0.4 < z < 1.1$ m	Radial field with $B_r \times B_z > 0$
Kicker field	$\lvert z \rvert < 0.4$ m	Radial pulsed field created by two pairs of round-type kicker coils.
Storage field	$r = 333 \pm 15$ mm, $z = \pm 50$ mm	Weak magnetic focusing, n-index $\sim (1.5 \pm 0.5) \times 10^{-4}$

Requirements for the magnetic field

Data Preprocessing & Implementation

NORMALIZATION

Spatial Coordinates

$$\tilde{x}, \tilde{y}, \tilde{z} = \frac{x}{L}, \frac{y}{L}, \frac{z}{L} \in [-1,1]$$

Coordinates scaled to [-1, 1]

Magnetic Field (Z-score)

$$\tilde{B} = \frac{B - \mu}{\sigma}$$

Components standardized using mean μ and std σ from training set. During inference: $\mathbf{B}_{\mathrm{pred}} = \tilde{\mathbf{B}}_{\mathrm{NN}} \times \boldsymbol{\sigma} + \boldsymbol{\mu}$

IMPLEMENTATION

Implemented in **PyTorch** with GPU acceleration for automatic differentiation. Enables continuous spatial reconstruction without grid-based discretization.

Workflow Overview

1. Surface Measurements

Collect B-field data on boundary points of the domain

2. Normalize & Train

Scale coordinates and fields, optimize PINN with three-stage training

3. Reconstruct Field

Query the trained network at arbitrary interior positions

4. Inverse Transform

Convert predictions back to physical units for validation

Three-Stage Training Strategy

01 AdamW Pre-training

First-order optimization with **decoupled weight decay**

- Rapidly navigates to global minimum neighborhood
- All losses converge by ~2 orders of magnitude
- Mitigates overfitting to sensor noise

→

02 LBFGS Fine-tuning

Second-order **quasi-Newton method**

- Exploits local curvature information
- Immediate refinement of solution
- Divergence loss drops below 10^{-5}

→

03 RAR Refinement

Residual-based Adaptive Refinement

- Evaluates residual $R = |\nabla \cdot B|$ and $|\nabla \times B|$ across dense probe points
- Adds high-residual points to collocation set
- Total loss driven below 10^{-7}

之江实验室 ZHEJIANG LAB

Biot-Savart Simulation Framework

SETUP

$$B(r) = \frac{\mu_0}{4\pi} \Sigma_i I_i \oint \frac{dl_i \times (r - r_i)}{| r - r_i |^3}$$

Synthetic environment with **multiple current-carrying circular loops** generating field within a cubic domain.

Case 1: Multi-loop (steep gradients, complex topology)

Case 2: Ideal Helmholtz pair (uniform field, contrast test)

Training data density sweep:

$N \in \{1, 3, 5, 9, 18\}$ points per face

→ 6 to 108 total surface measurements

Fixed Sampling / Random Sampling

Noise levels: 0.0%, 0.01%, 0.1%, 1.0%

Validation Framework

1. Analytical Biot-Savart solution provides reference field distribution (dimensionless framework)

2. Sample boundary points as "training data" — interior volume is independent validation set

3. Superimpose Gaussian noise $N(0, (\sigma B)^2)$ with $\sigma = \alpha|B|$ at varying levels

4. Evaluate reconstruction fidelity under divergence-free and curl-free constraints

Metric: Relative error = $(B_{pred} - B_{truth}) / B_{truth}$

之江实验室 ZHEJIANG LAB

Biot-Savart Simulation Framework

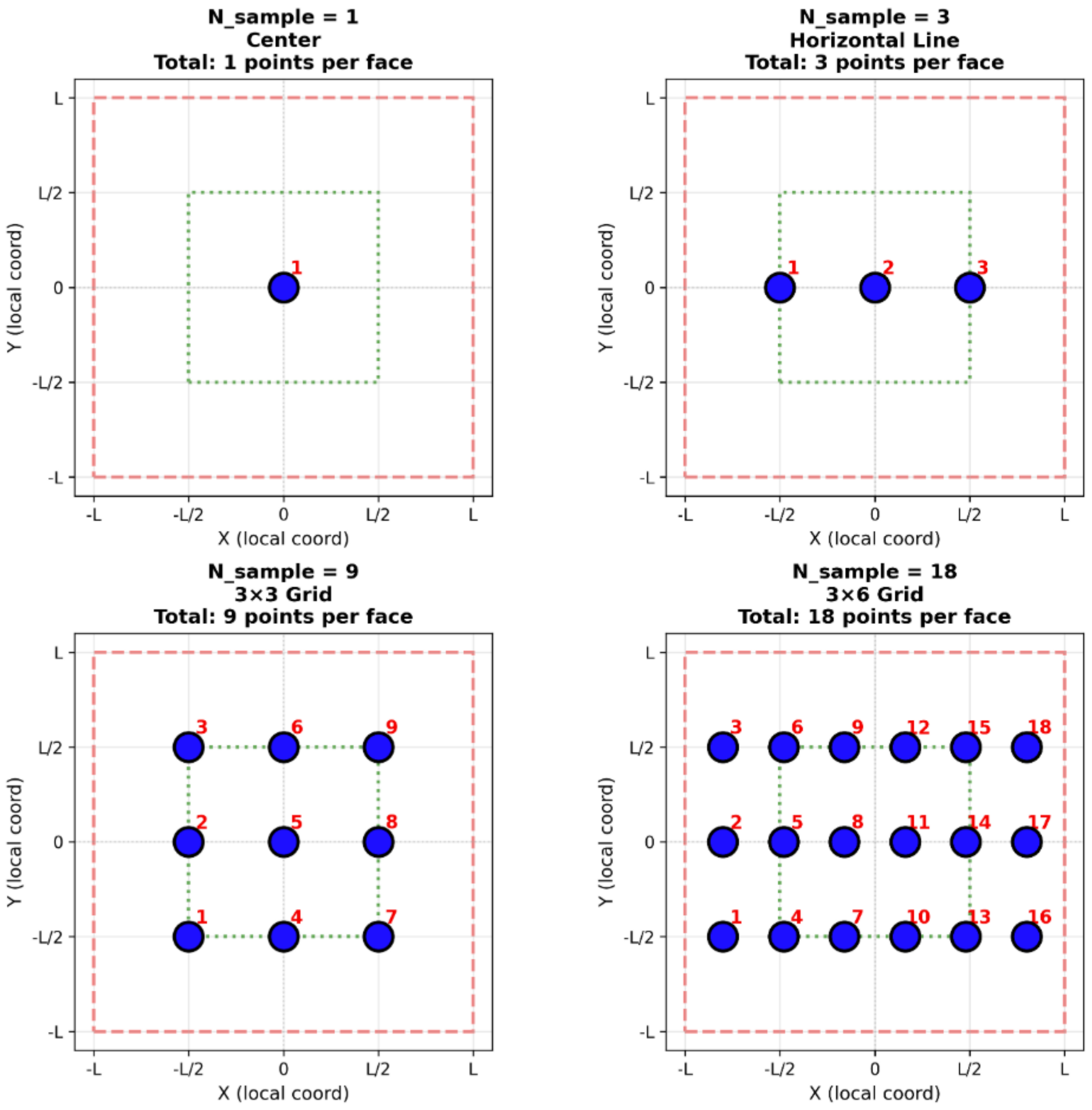

Training data density sweep:

N ∈ {1, 3, 5, 9, 18} points per face

→ 6 to 108 total surface measurements

Fixed Sampling / Random Sampling

Noise levels: 0.0%, 0.01%, 0.1%, 1.0%

Biot-Savart Simulation Result

- **Noise robustness:** PINN maintains 10^{-4} error across 0–1% noise; multipole degrades to 0.1–0.6%

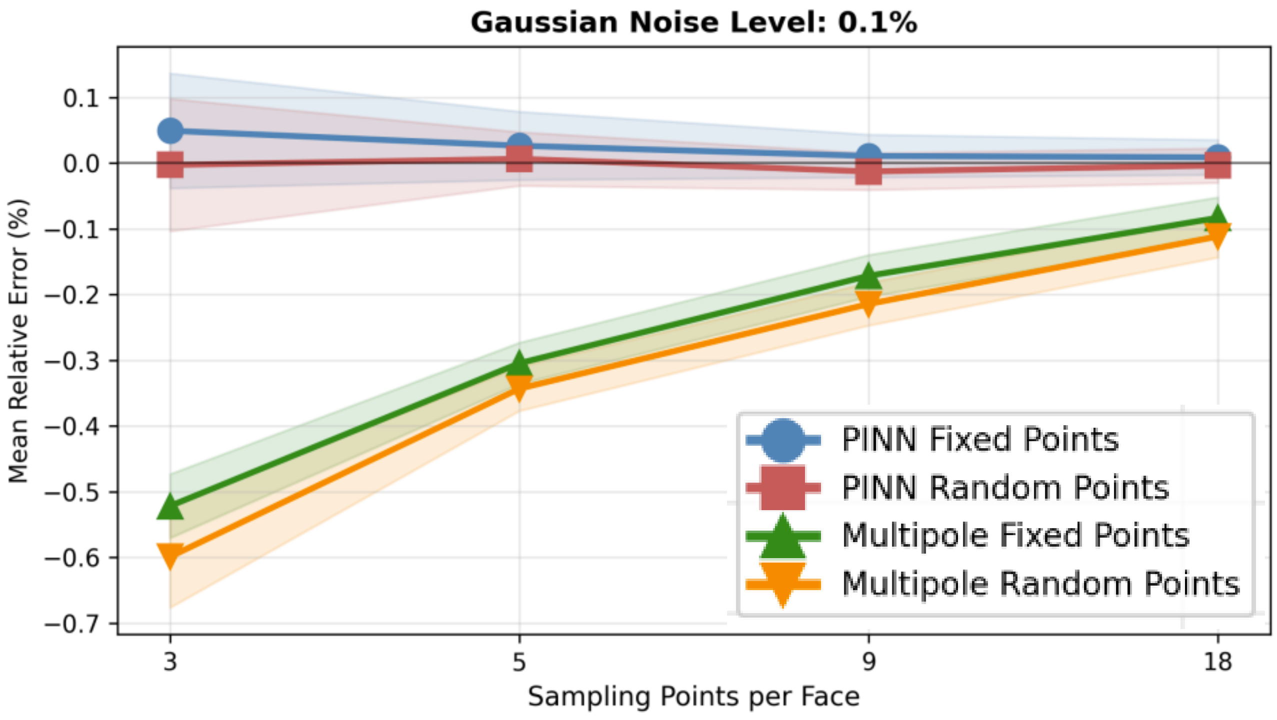

- **Sampling-insensitive:** PINN has flat accuracy from 3→18 points; multipole needs dense data
- **Physics regularization:** Built-in Maxwell constraints provide inherent regularization, eliminating truncation artifacts and the need for manual expansion-order tuning.

- Errors remain ~ 10^{-4} even at **1.0% noise**
- Weak dependence on sampling density (3→18 pts/face: <2×10^{-4} improvement)

之江实验室 ZHEJIANG LAB

Ablation study for experimental data

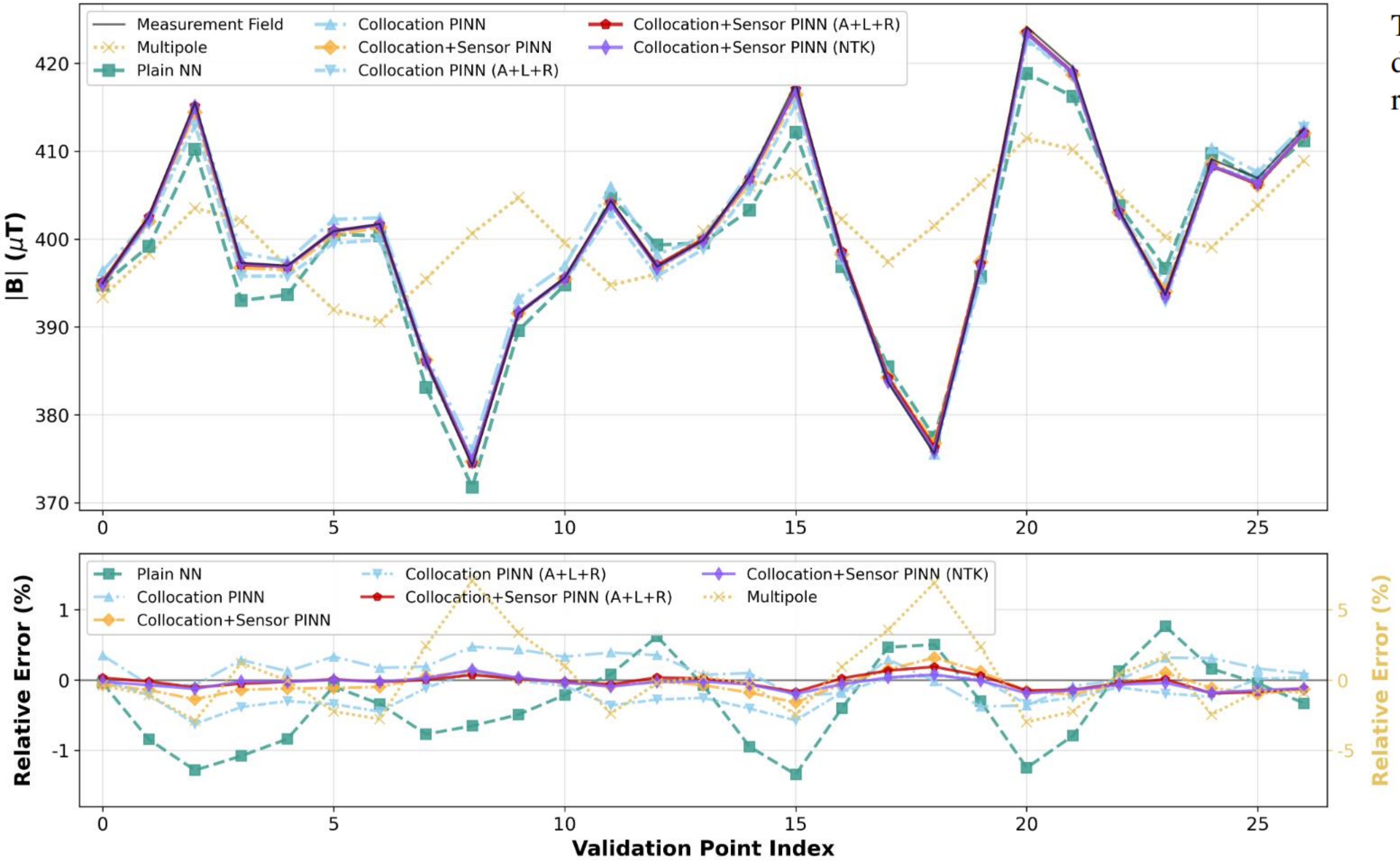

Table 2. Ablation study of PINN configurations on experimental data at $B_0 = 400\,\mu$T. A, L, and R denote the AdamW, LBFGS, and residual-based adaptive refinement stages, respectively.

Method	Rel. Err. (Mean±Std) (%)
Multipole	$+0.260 \pm 2.248$
Plain NN	-0.347 ± 0.581
Collocation PINN	$+0.127 \pm 0.235$
Collocation+Sensor PINN	-0.063 ± 0.137
Collocation PINN (A+L+R)	-0.199 ± 0.195
Collocation+Sensor PINN (A+L+R)	-0.027 ± 0.091
Collocation+Sensor PINN (NTK)	-0.049 ± 0.080